PROCEEDINGS OF ECOS 2023 - THE 36TH INTERNATIONAL CONFERENCE ON
EFFICIENCY, COST, OPTIMIZATION, SIMULATION AND ENVIRONMENTAL IMPACT OF ENERGY SYSTEMS
25-30 JUNE, 2023, LAS PALMAS DE GRAN CANARIA, SPAIN

Numerical simulation on thermal management of concentrating photovoltaic-thermal module with confined jet impingement with Ag-ZnO hybrid nanofluids

Abhishek Gupta[a], Sandesh S. Chougule[b], Sandip K. Saha[c]

[a] Department of Mechanical Engineering, Indian Institute of Technology Bombay, India, 204100029@iitb.ac.in

[b] Clean Energy Processes (CEP) Laboratory, Department of Chemical Engineering, Imperial College London, London SW72AZ, United Kingdom, s.chougule@imperial.ac.uk

[c] Department of Mechanical Engineering, Indian Institute of Technology Bombay, India, sandip.saha@iitb.ac.in

Abstract:

The high concentration of solar light on photovoltaic cells leads to extremely high cell temperatures, leading to decreased cell efficiency. Appropriate cooling techniques need to be integrated to sustain the high rise in temperature and maintain a uniform temperature throughout the photovoltaic cell. This study focuses on the cooling of photovoltaic cells with a confined jet impingement cooling technique. The major objective is to improve cell efficiency using the confined jet impingement technique to avoid hotspots, thermal stress, and current mismatching problem. The channels are created on the backside of the photovoltaic cell such that the coolant strikes the cell at the center and leaves at the four corners of the cell. Water-based ZnO and Ag-ZnO hybrid nanofluids are used as a coolant because of their high thermal conductivity and heat transfer capacity. The results showed better cooling performance and improved cell efficiency of photovoltaic cells with nanofluids compared to water as a coolant. In addition, sufficient temperature uniformity is maintained within PV cells. The effect of the coolant mass flow rate and nanoparticle volume concentration is also studied. Results showed improved cell electrical efficiency at higher coolant mass flow rates and higher nanoparticle volume concentration.

Keywords:

Concentrated photovoltaic; Confined jet impingement; Efficiency; Energy; Nano-fluids

1. Introduction

Solar energy is considered a significant renewable energy source. The annual potential of solar energy is 1,575–49,837 exajoules (EJ), which is 1.8–58 times the estimated future world energy consumption of 860 EJ in 2040 [1,2]. Solar energy can be used by various technologies such as photovoltaic (PV) systems, concentrated PV systems, solar thermal collectors, *etc*. PV systems and solar thermal collectors can be combined to obtain electrical and thermal energy outputs. Photovoltaic thermal (PVT) systems improve solar cell conversion efficiency, expanding solar energy utilization. However, the flat plate PVT system generates heat at low temperatures, which restrains the use of these systems for some high-temperature applications. To overcome such problems, concentrated photovoltaic thermal (CPVT) systems are a better alternative.

Concentrated photovoltaic (CPV) systems utilize optics to concentrate sunlight onto PV cells. Therefore, CPV can replace the expensive PV cells with cheaper concentrator optics to enable harnessing the same amount of solar radiation but with fewer PV receivers. Despite several advantages of a CPV system over flat plates, CPV systems face many challenges. The main challenge is that the high concentration of solar light on photovoltaic cells leads to extremely high cell temperatures, resulting in decreased cell efficiency. A major portion of the available solar energy is converted to thermal energy, leading to problems such as hotspots, current mismatching, and thermal fatigue. It is essential to have a uniform PV cell temperature to avoid current mismatching and thermal stresses. To sustain the high rise in temperature and to maintain a uniform

https://doi.org/10.52202/069564-0050

temperature throughout the photovoltaic cell, appropriate cooling techniques are required to be integrated. Many cooling techniques, such as air-based cooling, liquid immersion, jet impingement, phase change material cooling, heat pipe, micro-channel cooling, and thermoelectric cooling, have been employed, which were reviewed in various literature [3]. Theristis et al. [4] reported that passive cooling is not enough to dissipate heat from the cell under high concentration ratios. Jet impingement is an appropriate cooling method for densely packed PV cells to achieve a uniform cell temperature [5]. Many researchers reviewed unconfined and confined jet impingement cooling systems for PV cells. Recent studies showed that the temperature of the PV cell can be reduced from 1360 °C to 65 °C for a concentration ratio of 1000 suns using confined jet impingement cooling with water at a mass flow rate of 50 g/min [6]. Javidan et al. [7] reported that temperature of the PV module decreased from 63.95 °C to 33.68 °C by using an optical set of parameters for jet impingement cooling. Bahaidarah et al. [8] reported a temperature decrease from 69.7 °C to 36.6 °C using an unconfined jet impingement cooling technique. Zubeer et al. [9] reported that the temperature of an uncooled PV system and a low-concentrated (1-3 suns) PV system was 57.5 °C and 64.1 °C, respectively, which decreased to 36.5 °C with water jet impingement cooling. Barrau et al. [10] studied the performance of hybrid jet impingement micro-channel cooling for densely packed PV cells, and calculated the heat transfer coefficient as a function of pressure drop, and compared the performance of hybrid cooling to micro-channel cooling alone. Markal et al. [11] performed experiments to investigate the effect of impinging air jets on the cooling of PV cells. It was found that the average surface temperature of the PV cell can be decreased by 61.5%, and the output power can be improved by 13.2%. Amanlou et al. [12] studied the effect of air diffuser geometry on the performance of low-concentrated PV systems. Also, the effect of air mass flow rates on concentrated PV cells' performance was studied. It is reported that by increasing the air mass flow rate from 0.0008 to 0.016 kg/s, the electrical, thermal, and overall efficiency of the PV cell was improved by 13.5, 22.75, and 22.41%, respectively. Singh et al. [13] performed numerical modelling and experimental study for performance improvement of PV modules with a hybrid cooling system with a thermoelectric cooler and phase change material. It was reported that TECs provide better cooling than PCMs under similar conditions as panel efficiency increases by 5.73%. It was observed that electrical efficiency shows a maximum increment of 19.4% with hybrid cooling. Sabry et al. [14] studied thermoelectric generator (TEG) cooling on concentrated PV systems. Compared to only a CPV cell on top of a heat sink, the generated power of the CPV/TEG hybrid system increased by 7.4%, 5.8%, and 3% corresponding to using the 30 × 30 mm^2, 40 × 40 mm^2 and the 62 × 62 mm^2 TEG modules, for which the number of junctions is 31, 127 and 49, respectively.

The aim is to design a highly efficient CPVT system with hybrid cooling, such as confined jet impingement and a thermoelectric generator. Although many researchers have worked on the performance of jet impingement cooling of microelectronics, very few studies are reported on confined jet impingement cooling of highly concentrated PV systems. Confined jet impingement cooling provides a better uniform PV cell temperature, eliminating thermal stresses and current mismatching. Most researchers use water as a cooling fluid for jet impingement cooling of PV cells. Nanofluids provide better cooling than water because of their higher thermal conductivity [15]. In this work, the performance improvement of a highly concentrated PV system under confined jet impingement with Ag-ZnO hybrid nanofluids as a coolant is studied. The effect of volume concentration of Ag-ZnO nanoparticles on CPV cell cooling and electrical efficiency is observed. Also, the effect of the mass flow rate of the Ag-ZnO hybrid nanofluid on the performance of confined jet impingement cooling of CPV cell is studied, and the performance of Ag-ZnO hybrid nanofluids is compared with water as a cooling fluid.

2. System description

2.1 System Geometry

The solar cell used in this analysis is a multi-junction solar cell with a reference cell efficiency of 40.3% at a reference temperature of 298 K. The dimension of the solar cell is 10 mm × 10 mm with 0.19 mm thickness. The solar cell is supported by a board structure which consists of a copper structure followed by a ceramic and copper board. The upper copper layer's dimensions are 24 mm × 19.5 mm with 0.25 mm thickness, followed by a 25.5 mm × 21 mm ceramic layer and a 25 mm × 20.5 mm copper layer with 0.32 mm and 0.25 mm thickness, respectively. An aluminium heat sink of 25.5 mm × 21 mm with 4 mm height is placed at the bottom of the structure. An inlet is placed at the center of the heat sink, and four outlets are placed at the four corners. The cooling fluid enters the center of the heat sink and exits through the four outlets at the corner.

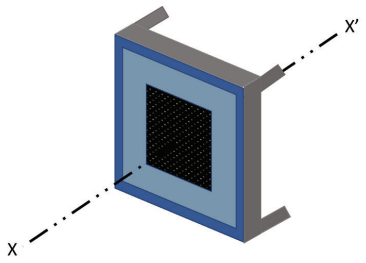

(a)

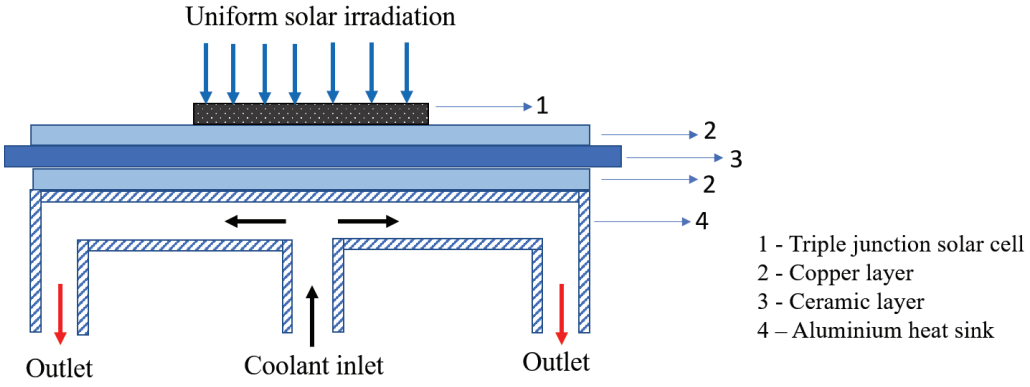

(b)

Figure 1. (a) Isometric view of the assembly (b) Solar cell layers and jet impingement channel configuration.

Table 1. Properties of solar cell layers and board structure

Solar cell layer	Thermal conductivity (k) (W/m.K)	Specific heat (C) (J/kg.K)	Density (ρ) (kg/m^3)	Emissivity (ε)
Germanium	60	320	5323	0.9
Copper-1	400	385	8700	0.05
Ceramic	30	900	3900	0.75
Copper-2	202.6	871	2719	0.9

2.2 Governing equations

For solar cell layers:

The heat conduction equation between the layers of the PV cell is as follows:

$$\nabla(k_i \nabla T_i) + q_i = 0 \quad (1)$$

where k_i represents the thermal conductivity of the ith layer.

Internal heat generation term is added for the germanium layer because heat is generated inside the germanium layer due to solar radiation absorption.

The heat generated in the germanium layer is calculated according to the following expression:

$$q_{Ge} = \frac{(1-\eta_{cell}).G.\alpha_{Ge}.A}{V} \quad (2)$$

https://doi.org/10.52202/069564-0050

where *G* is the net concentrated solar irradiation, *α* is the absorptivity of the germanium layer, and *A* and *V* are the surface area and volume of the germanium layer, respectively. η_{cell} is the cell's electrical efficiency.

The net concentrated solar irradiation is a function of the optical efficiency of the solar cell (η_{opt}) and the concentration ratio (CR) of the solar cell.

$$G = I.CR.\eta_{opt} \quad (3)$$

where *I* is the solar irradiation falling on the solar cell.

The electrical efficiency of the solar cell (η_{cell}) is a function of the operating temperature of the solar cell. As the temperature of the solar cell increases, the cell efficiency decreases. The term (1-η_{cell}) represents the portion of absorbed concentrated solar irradiance converted to heat. This heat has to be dissipated or absorbed by the coolants to keep the cell's temperature low. The solar cell's electrical efficiency is expressed in terms of the operating temperature of the cell by the following equation:

$$\eta_{cell} = \eta_{ref} - \beta_{thermal}(T_{cell} - T_{ref}) \quad (4)$$

where cell reference efficiency η_{ref} is taken as 40.3% at reference temperature T_{ref} = 298K and CR = 1000, and $\beta_{thermal}$ is the thermal coefficient and is equal to 0.047%.

For jet impingement:

Continuity equation:

$$\nabla.\left(\rho_f \vec{V}\right) = 0 \quad (5)$$

Momentum equation:

$$\vec{V}.\nabla\left(\rho_f \vec{V}\right) = -\nabla P + \nabla.(\mu_f \nabla \vec{V}) \quad (6)$$

Energy equation:

$$\vec{V}.\nabla\left(\rho_f C_f T\right) = \nabla.(k_f \nabla T) \quad (7)$$

where, ρ, μ and *k* are the density, viscosity, and thermal conductivity of the coolant fluid, respectively. $\vec{V}$ and *P* is the velocity and pressure, respectively.

2.3 Boundary conditions:

The top layer of the concentrated PV system is subjected to mixed convection radiation heat losses boundary conditions. All of the sides of the CPV system are given adiabatic boundary conditions. For the coolant, inlet jets are given uniform temperature and velocity normal to the inlet boundary conditions, and at the outlet, zero-gauge pressure boundary condition was given.

For the top layer of the germanium cell layer and copper layer:

$$-k_{Ge}\frac{\partial T_{Ge}}{\partial z} = q_{rad,Ge\to S} + q_{conv,Ge\to a} \quad (8)$$

$$-k_{cu}\frac{\partial T_{cu}}{\partial z} = q_{rad,cu\to S} + q_{conv,cu\to a} \quad (9)$$

where, $q_{rad,Ge\to S}$ is the radiative heat loss from the Germanium layer to the sky and $q_{conv,Ge\to a}$ is the convective heat loss from the germanium layer to the ambient.

The convective heat loss from the Germanium layer to the ambient can be calculated using the following correlations:

$$q_{conv,Ge\to a} = h_{conv,wind}(T_{Ge} - T_a) \quad (10)$$

$$h_{conv,wind} = 5.82 + 4.07V_{wind} \quad (11)$$

where T_a is the ambient temperature, T_{Ge} is the temperature of the Germanium cell, $h_{conv,wind}$ is the convective heat transfer coefficient, and V_{wind} is the wind velocity.

Radiation heat loss from the germanium layer to the sky can be calculated using the following expression:

$$q_{rad,Ge\to S} = \sigma\epsilon_{Ge}(T_{Ge}^4 - T_s^4) \quad (12)$$

$$T_s = 0.0522T_a^{1.5} \quad (13)$$

where ε_{Ge} is the emissivity of Germanium, T_s is the sky temperature in Kelvin, and T_a is the ambient temperature in Kelvin.

At the interfaces between all layers, thermally coupled boundary conditions are given. At the interface between the germanium layer and copper top layer, the thermally coupled boundary condition is given as follows:

$$-k_{Ge}\nabla T_{Ge} = -k_{cu}\nabla T_{cu} \quad (14)$$

$$T_{Ge} = T_{cu}$$

At the interface between the top copper layer and the ceramic layer:

$$-k_{cu}\nabla T_{cu} = -k_{ce}\nabla T_{ce} \quad (15)$$

$$T_{cu} = T_{ce}$$

At the interface between the ceramic layer and the bottom copper layer:

$$-k_{ce}\nabla T_{ce} = -k_{cu,b}\nabla T_{cu,b} \quad (16)$$

$$T_{ce} = T_{cu,b}$$

At the interface between the bottom copper layer and the heat sink top surface:

$$-k_{cu,b}\nabla T_{cu,b} = -k_{Al}\nabla T_{Al} \quad (17)$$

$$T_{cu,b} = T_{Al}$$

where T_{Ge}, T_{cu}, T_{ce}, $T_{cu,b}$, T_{Al} are the temperatures of the germanium cell layer, top copper layer, ceramic layer, bottom copper layer, and aluminium heat sink, respectively. k_{Ge}, k_{cu}, k_{ce}, $k_{cu,b}$, k_{Al} are the thermal conductivities of the germanium cell layer, top copper layer, ceramic layer, bottom copper layer, and aluminium layer, respectively.

For heat sink inlets and outlets:

At inlet: $V_f = V_{in}$ and T_{in} = 298K

At outlet: gauge pressure P_{out} = 0

All sides of the heat sink wall and the back side are adiabatic.

No slip boundary condition at the fluid-solid interface.

3. Results and discussion

3.1 Validation

The present numerical model is validated with Zahhad et al. [6]. The authors investigated the variation in cell temperature with a mass flow rate of cooling fluid and concentration ratio. The authors studied the variation in thermal stress along the center and diagonal lines of the cell. Zahhad et al. [6] used water as a cooling fluid. Figure 2 shows the variation in the temperature of the Germanium cell with respect to the inlet mass flow rate of the cooling fluid. It is observed that the cell temperature decreases with an increase in the coolant mass flow rate. The configuration with one inlet at the center is better than multiple inlet jets because of the absence of cross-flow. Therefore, the impingement zone develops without restrictions at the target surface of the impinging. A reasonable agreement is found between the present numerical model and the results by Zahhad et al. [6]. An average error of 1.68% and an average temperature difference of 1.33 K is found between the present numerical model and the results by Zahhad et al. [6].

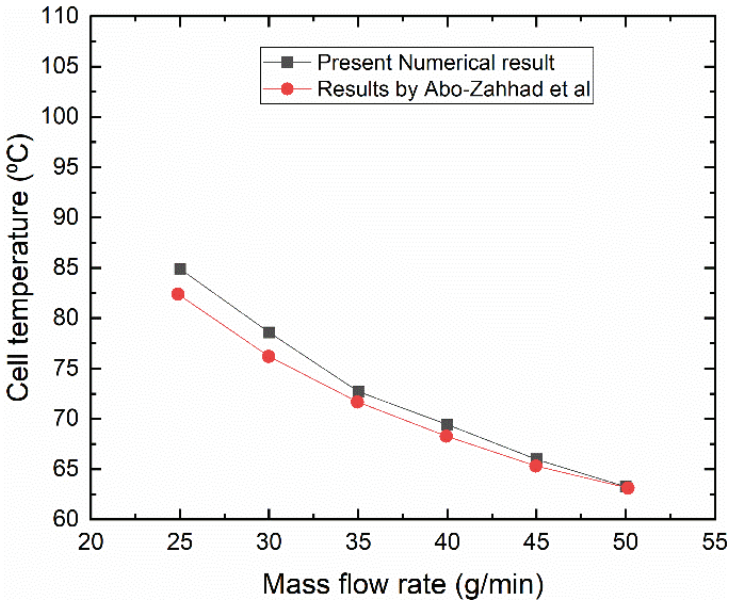

Figure 2. Validation of numerical model with Zahhad et al. [6].

https://doi.org/10.52202/069564-0050

The simulation is further performed for the same configuration with Ag-ZnO hybrid nanofluids as a cooling fluid. The thermophysical properties used for Ag-ZnO hybrid nanofluids are listed below [15] :

Table 2. Thermophysical properties of Ag-ZnO hybrid nanofluids

Volume concentration (%)	Density (kg/m^3)	Specific heat (J/kg-K)	Thermal conductivity ratio (K_{nf}/K_b)	Viscosity (Pa-s)
0.02	1000.932	4186.264	1.08	0.0031
0.04	1001.864	4185.527	1.145	0.0035
0.06	1002.796	4184.791	1.185	0.0042
0.08	1003.728	4184.054	1.25	0.0045
0.10	1004.66	4183.318	1.29	0.0052

Figure 3 shows the cell temperature at varying volume concentrations of Ag-ZnO nanoparticles at a mass flow rate of 25 g/min. The cell temperature decreases with an increase in the volume concentration of nanoparticles. This is because of the enhanced thermophysical properties of nanofluids at a higher volume concentration of nanoparticles. The thermal conductivity of nanofluids increases due to the Brownian motion of nanoparticles. Nanoparticles move through the liquid, and convection is induced due to the Brownian motion of nanoparticles. This leads to an increase in nanofluid thermal conductivity. Also, the ballistic phonon transport of nanoparticles helps increase the thermal conductivity of nanofluids. Due to the increase in the thermal conductivity of nanofluids, the amount of heat transferred from the bottom copper layer to the coolant increases.

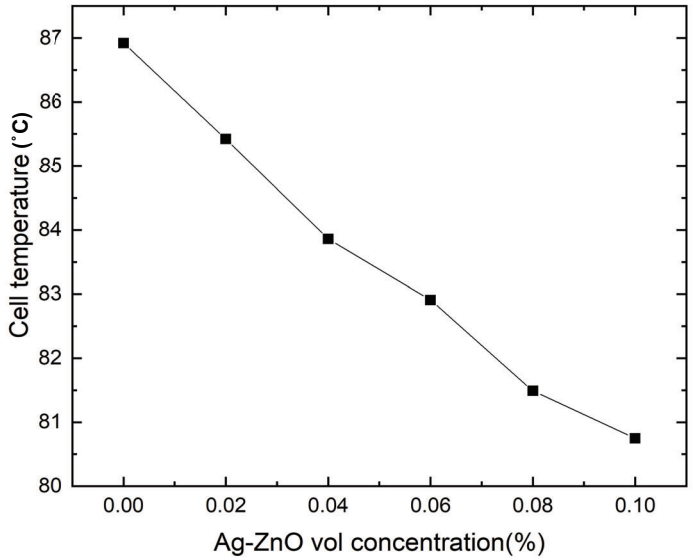

Figure 3. Variation in cell temperature with Ag-ZnO volume concentration.

Figure 4 shows the cell electrical efficiency with a varying volume concentration of Ag-ZnO nanoparticles at a mass flow rate of 25 g/min. It is evident that the electrical efficiency increases with increasing nanoparticle volume concentration. Since the cell temperature decreases with an increasing volume concentration of nanoparticles, the cell's electrical efficiency increases.

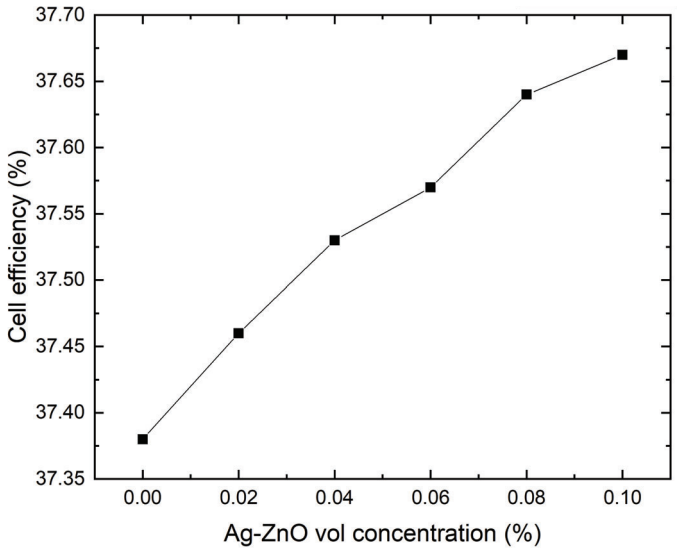

Figure 4. Variation in cell electrical efficiency with Ag-ZnO volume concentration.

Figure 5 shows the effect of the mass flow rate of Ag-ZnO nanofluids at 0.1% volume concentration on the average cell temperature and compares it with water as a coolant. The minimum mass flow rate is 25 g/min to avoid flow boiling. It is observed that Ag-ZnO hybrid nanofluids cool the cell better because of their enhanced thermophysical properties. Therefore, the cell's electrical efficiency will be higher with nanofluids as a cooling fluid.

Although cell temperature decreases at higher coolant mass flow rates, the pressure drop also increases with the increase in the coolant mass flow rate. The net power gained is affected by frictional pressure drops. To use waste heat from highly concentrated PV system applications, the coolant mass flow rate should be low.

Cell temperature variation on the cell surface is also evaluated. It is observed that the maximum temperature difference at the surface of the cell is 2.06 °C for a mass flow rate of 25 g/min at 0.1% volume concentration of Ag-ZnO nanoparticles. It shows that temperature uniformity can be achieved using a confined jet impingement cooling technique on the surface of the PV cell. This will eliminate the problems associated with thermal stresses and current mismatching.

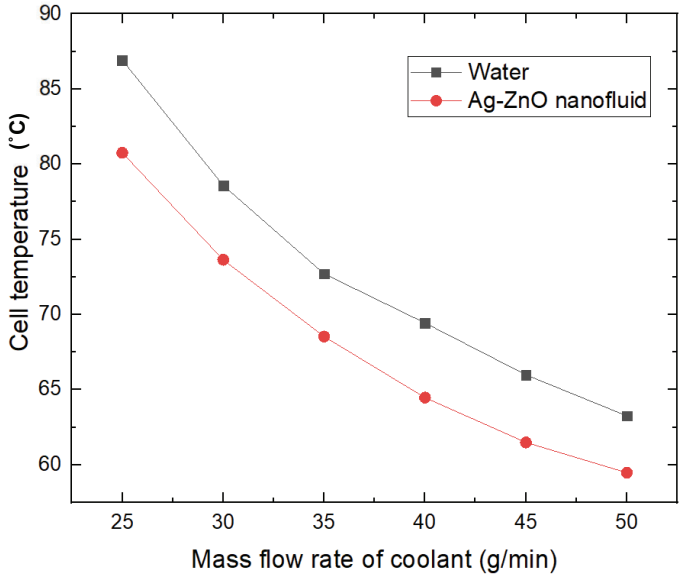

Figure 5. Variation in cell temperature with mass flow rate of coolant.

https://doi.org/10.52202/069564-0050

4. Conclusions

It is found that Ag-ZnO hybrid nanofluids can perform a better cooling of the cell than water because of the enhanced thermophysical properties of nanofluids. The thermal conductivity of nanofluids increases compared to base fluid, which increases heat transfer from the bottom copper layer to the coolant. The higher the nanoparticle volume concentration, the better the cooling effect. Also, nanofluids will increase cell electrical efficiency. It is observed that numerically there is only a slight increase in cell efficiency with nanofluids compared to water. Experiments with the proposed system will be performed in the future. Surely, the cooling of CPV cells and cell electrical efficiency will be improved in experimentation since the effect of Brownian motion and ballistic transport phonon of nanoparticles will be observed in experiments.

Nomenclature

A	area of the solar cell, m^2
CR	concentration ratio
G	concentrated solar irradiance, W/m^2
h	convective heat transfer coefficient, $W/(m^2\ K)$
I	direct normal irradiation, W/m^2
k	thermal conductivity, W/(m K)
L	length, m
$\dot{m}$	mass flow rate of coolant, kg/s
q	heat flux, W/m^2
T	temperature, ˚C
V	volume of solar cell, m^3
v	velocity, m/s
W	width, m

Greek symbols

μ	Viscosity, Pa s
α	absorptivity
$\beta_{thermal}$	solar cell temperature coefficient
Δ	difference
δ	thickness, m
η	efficiency, %
ρ	density, kg/m^3
σ	Stefan-Boltzmann constant, 5.67×10^{-8} $W/(m^2\ K^4)$

Subscripts and superscripts

a	ambient
b	base fluid
cell	for cell layer
conv	convection
cu	copper layer
f	fluid
Ge	germanium layer
in	inlet
nf	nanofluid
opt	optical
out	outlet
rad	radiation
ref	reference

Abbreviations

CPV	concentrated photovoltaic
CPVT	concentrated photovoltaic thermal
HCPV	high concentrated photovoltaic

PV photovoltaic

TEC Thermoelectric coolers

TEG Thermoelectric generator

References

1. World energy assessment. United Nations Development Programme; 2000.
2. International energy outlook 2016 with projections to 2040. U.S. Energy Information Administration; 2016.
3. Dwivedi P, Sudhakar K, Soni A, Solomin E, Kirpichnikova I. Advanced cooling techniques of P.V. modules: A state of art. Case Stud Therm Eng [Internet]. 2020;21(December 2019):100674. Available from: https://doi.org/10.1016/j.csite.2020.100674
4. Theristis M, O'Donovan TS. Electrical-thermal analysis of III-V triple-junction solar cells under variable spectra and ambient temperatures. Sol Energy [Internet]. 2015;118:533–46. Available from: http://dx.doi.org/10.1016/j.solener.2015.06.003
5. Royne A, Dey CJ. Design of a jet impingement cooling device for densely packed PV cells under high concentration. Sol Energy. 2007;81(8):1014–24.
6. Abo-Zahhad EM, Ookawara S, Radwan A, El-Shazly AH, ElKady MF. Thermal and structure analyses of high concentrator solar cell under confined jet impingement cooling. Energy Convers Manag [Internet]. 2018;176(September):39–54. Available from: https://doi.org/10.1016/j.enconman.2018.09.005
7. Javidan M, Moghadam AJ. Experimental investigation on thermal management of a photovoltaic module using water-jet impingement cooling. Energy Convers Manag. 2021;228(October 2020).
8. Bahaidarah HMS. Experimental performance evaluation and modeling of jet impingement cooling for thermal management of photovoltaics. Sol Energy [Internet]. 2016;135:605–17. Available from: http://dx.doi.org/10.1016/j.solener.2016.06.015
9. Zubeer SA, Ali OM. Experimental and numerical study of low concentration and water-cooling effect on PV module performance. Case Stud Therm Eng [Internet]. 2022;34(September 2021):102007. Available from: https://doi.org/10.1016/j.csite.2022.102007
10. Barrau J, Rosell J, Chemisana D, Tadrist L, Ibañez M. Effect of a hybrid jet impingement/micro-channel cooling device on the performance of densely packed PV cells under high concentration. Sol Energy. 2011;85(11):2655–65.
11. Markal B, Varol R. The Effect of Jet Impingement on the Performance of a Photovoltaic Module. 2019;4(1):647–50.
12. Amanlou Y, Tavakoli Hashjin T, Ghobadian B, Najafi G. Air cooling low concentrated photovoltaic/thermal (LCPV/T) solar collector to approach uniform temperature distribution on the PV plate. Appl Therm Eng. 2018;141(May):413–21.
13. Singh D, Chaubey H, Parvez Y, Monga A, Srivastava S. Performance improvement of solar PV module through hybrid cooling system with thermoelectric coolers and phase change material. Sol Energy [Internet]. 2022;241(June):538–52. Available from: https://doi.org/10.1016/j.solener.2022.06.028
14. Sabry M, Lashin A, Al Turkestani M. Experimental and simulation investigations of CPV/TEG hybrid system. J King Saud Univ - Sci [Internet]. 2021;33(2):101321. Available from: https://doi.org/10.1016/j.jksus.2020.101321
15. Barewar SD, Chougule SS, Jadhav J, Biswas S. Synthesis and thermo-physical properties of water-based novel Ag/ZnO hybrid nanofluids. J Therm Anal Calorim [Internet]. 2018;134(3):1493–504. Available from: https://doi.org/10.1007/s10973-018-7883-6

https://doi.org/10.52202/069564-0050